Effects of Sunshine UV Irradiation on the Tensile Properties and Structure of Ultrahigh Molecular Weight Polyethylene Fiber

Huapeng Zhang,[1] Meiwu Shi,[2] Jianchun Zhang,[2] Shanyuan Wang[1]

[1]*Textile College of Donghua University, 200051 Shanghai, China*
[2]*Soldier Center of the Quartermaster Institute of the General Logistics of PLA, 100088 Beijing, China*

Received 4 September 2002; accepted 29 October 2002

ABSTRACT: This study investigated sunlight-simulated ultraviolet (UV) beam irradiation on the tensile properties and structure of ultrahigh molecular weight polyethylene (UHMWPE) fibers. The tensile results showed that after 300 h sunlight UV irradiation, the tensile properties of the UHMWPE fibers were obviously degraded. Investigation of morphology revealed that the crystallinity was slightly increased, whereas the overall orientation and molecular weight of the fibers were decreased. SEM observations indicated that the degradation process was nonuniform throughout the fiber and a change from a ductile to a brittle fracture mechanism was found after UV irradiation. DMA results showed two β-relaxations and one α-relaxation in the original single filament, and UV irradiation led to the increased intensity of the high-temperature β-relaxation and the lowered position of the low-temperature β-relaxation. This indicated that irradiation-induced molecular scission and branching were located primarily in the amorphous and the interface areas of the fiber. Changes in the thermal behavior were also examined by DSC. © 2003 Wiley Periodicals, Inc. J Appl Polym Sci 89: 2757–2763, 2003

Key words: UHMWPE fibers; mechanical properties; structure; UV irradiation; thermal properties

INTRODUCTION

In theory ultrahigh molecular weight polyethylene (UHMWPE) fibers should be sunlight stable on the basis of the fact that pure UHMWPE absorbs no radiation of wavelengths longer than 190 nm,[1] and 290 nm may be taken as the shortest wavelength (highest energy) radiation present in the UV spectrum of the sun at the ground level. However, internal and/or external impurities (very often containing UV/light-absorbing chromophoric groups such as hydroperoxides, carbonyls, and unsaturated bonds[2,3]) are formed perhaps during polymerization processes and further processing and storage,[4] which can change the absorbing wavelength up to 270–330 nm and initialize primary oxidative reactions.[5] Many reports on the photodegradation and oxidation of UHMWPE products other than fibers have been published, especially in the orthopedic industry where the UHMWPE is γ- or electron beam irradiated to sterilize prostheses, or to crosslink the UHMWPE to improve creep or thermal-resistance behaviors.[6–8] Numerous investigations indicated that high energy beam–induced degradation was diffusion controlled in solid polymers, and oxidation first took place on the surface and then progressed into the inner portion. Besides, because of the difference of oxygen diffusion and solubility between the amorphous and crystalline domains, oxidation was first initiated in the amorphous domains, leading to the molecule scission and/or crosslinking of these zones and further changes of the properties, structure, and morphology of the irradiated material.

Mechanical properties are of critical importance in engineering, especially for high-performance UHMWPE fibers, which are acclaimed for their high modulus and tenacity. Despite the low amorphous fraction of UHMWPE fibers, attributed to their high surface-to-volume specific ratio, the deterioration of tensile properties and structure of UHMWPE fibers after sunlight irradiation cannot be ignored; and considering UHMWPE's supposed good light resistance, to our knowledge there are only a few reports on the effects of UV irradiation on the tensile properties and structure of UHMWPE fibers. The objectives of the present work were to investigate the tensile property and structural changes of UHMWPE filaments with sunlight-simulated UV irradiation, and the implications on the complex morphologies of UHMWPE fibers.

EXPERIMENTAL

Sample preparation

The UHMWPE fiber used in this study was the Dyneema SK65 UHMWPE fiber manufactured by

Correspondence to: H. Zhang (roczhp@163.com).

Journal of Applied Polymer Science, Vol. 89, 2757–2763 (2003)

DSM (The Netherlands), which has tenacity of 3.0 cN/dtex, modulus of 96 cN/dtex, and breaking extension of 3.6% with no twist, according to the manufacturer. The filament yarn was carefully unreeled from the Dyneema SK65 bobbin, and then the continuous filaments were wound in a parallel manner onto a steel frame whose size was suitable for mounting into the irradiation equipment. Much care was taken to spread the filaments in the yarn as uniformly and as wide as possible to prevent screening effects. A UV Auto Fade Meter U48 AU instrument was adopted to irradiate the specimens. The sunshine carbon arc lamp emitted a UV beam of wavelength ranging from 350 to 420 nm, with emission peaks at 360, 380, and 390 nm. The temperature and humidity in the irradiation chamber were 40 ± 3°C and 45%, respectively.

Measurements and characterizations

The tenacity, modulus, break extension, and work to break of the original and irradiated yarns were recorded by an Instron 4466 tensile tester by adopting the Instron yarn-gripping attachment with nominal gauge length of 50 cm (from the upper edge to the lower edge of the grippers), and the crosshead speed was set at 50 cm/min. The moduli of the yarns were the tangent moduli derived from the stress–strain curves at 0.5% strain. All tensile tests were carried out at ambient conditions, with constant temperature and humidity; the sample size of every test was chosen to ensure ±10% variance at 90% confidence level. A JSM-5600LV SEM was used to observe the surfaces and fractured ends of the single filaments.

The filaments before and after irradiation were dissolved in decalin, at 0.1% concentration, for 2 h at 150°C; the intrinsic viscosity was measured at 135°C by dilution viscometry in an Ubbelohde viscometer. The weight-average molecular weight was converted from the intrinsic viscosity [η] by the relationship [η] = $6.77 \times 10^{-4}[M_w]^{0.67}$.[9]

The intensity profiles of the UHMWPE filaments before and after irradiation were measured with Ni-filtered Cu–K_α irradiation (l = 1.54 Å) using a Rigaku D/Max-3AX WAXD diffractometer (Rigaku, Tokyo, Japan) with a fiber-specimen holder. The parallel multifilament yarn was bundled and fixed onto the X-ray sample holder (10 mm wide, 10 mm long). The X-ray beam was perpendicular to the bundle plane. The data were collected over the 2θ range from 17 to 28° and the scan rate was 1°/min. The separation of overlapping reflections was performed with a peak-fitting program after various intensity corrections, taking the crystalline peaks as Gaussian curves and the amorphous halo centered around 23°.[10] From the fully corrected and resolved peak profiles the relative crystallinity (crystalline index, *CI*) was determined by eq. (1)[11] and crystallite size was calculated by the Scherrer eq. (2).[12]

$$CI = 1 - \frac{A_a}{A} \tag{1}$$

$$L_{(hkl)} = \frac{K\lambda}{\delta \cos \theta} \tag{2}$$

where A_a is the diffraction area of the amorphous area obtained by peak fitting; A is the total diffraction area of the corrected intensity profile in eq. (1); $L_{(hkl)}$ is the weight-average size of a crystallite perpendicular to its diffracting planes; K is a coefficient related to the crystallites' structures and the definitions of $L_{(hkl)}$ and δ, and is always taken as 0.9 when δ is the full width at half maximum (FWHM) and 1.0 when δ is the integral breadth; θ is half of the Bragg angle 2θ; λ is the wavelength of Cu–K_α beam; here δ is the FWHM of the respective crystalline peaks.

An assessment of crystalline orientation H, the half-height width along the azimuthal direction, was obtained by measurements on the equatorial (110) reflections with Ni-filtered Cu–K_α irradiation using a Rigaku D/Max-3AX WAXD diffractometer. The data were collected over the azimuthal angle φ range from 50 to 120° at 5°-increments. A qualitative measure of the crystalline orientation factor π was carried out by use of eq. (3), as follows[13]:

$$\pi = \frac{180 - H}{180} \times 100 \tag{3}$$

The chain orientation factor of sonic velocity was determined by measuring the transmitting time of a sound between two transducers coupled to the specimens. The measurements were made by use of an SCY-III model fiber sonic velocity meter. From the measured sonic velocity C, the chain orientation factor of samples f was calculated by eq. (4):

$$f = 1 - (c_u/c)^2 \tag{4}$$

where c_u is the sonic velocity of the fully unoriented sample, taken as 1.65 km/s.[14]

Thermal analysis was conducted using a Perkin–Elmer Pyris 1 DSC (Perkin Elmer Cetus, Norwalk, CT), which was calibrated against the melting of high-purity indium. Fibers were cut into short lengths and 5–6 mg of fiber was crimped into a standard aluminum sample pan. The samples were heated at a constant rate of 10°C/min.

The tan δ–temperature relationship of a single filament was obtained by Rheometric Scientific DMAIV with the cylinder/fiber compression/tension geometry type, dynamic temperature ramp test type, and static force tracking dynamic force mode (with the former more than the latter by 2.0%), at a frequency of 1 Hz, a temperature ramp rate of 5°C/min from −150

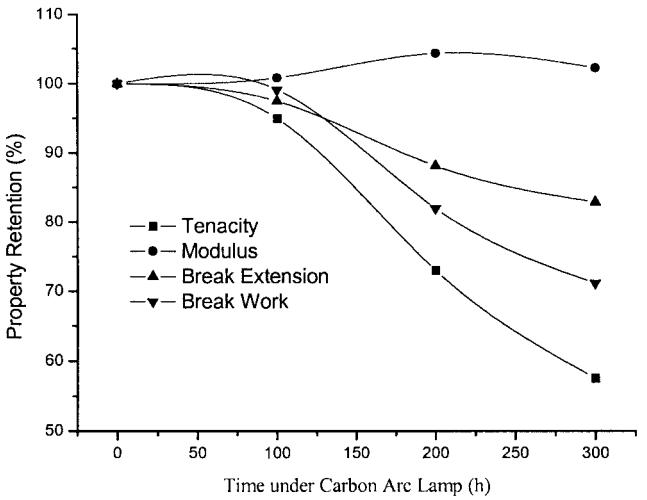

Figure 1 Plot of tensile properties versus irradiation time.

to 130°C, and a controlled strain of 0.3%. All tests were repeated three times to ensure reproducibility and the typical results were chosen for analysis.

RESULTS AND DISCUSSION

Effects of UV irradiation on the tensile properties of UHMWPE filaments

From Figure 1, we see that with irradiation the tenacity, break extension, and work to break of the filaments decrease, although the rates of decrease are not constant. The modulus of the filaments increases slightly with irradiation, which is in line with the report that the UHMWPE fiber was oxidized by potassium dichromate.[15] The results suggest that, when the filament is irradiated by sunlight-simulated UV beam, chain scission and crosslinking occur simultaneously. Chain scission leads to the deterioration of tenacity, break extension, and work to break, but crosslinking leads to the increase of modulus.

Figure 2 shows that after UV irradiation the surface

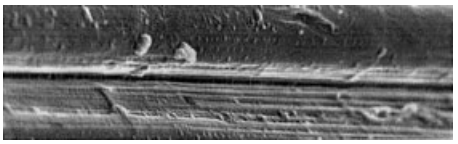

Figure 3 Close-up of area A in Figure 2(b).

of the filaments become rough and corrugated, and there are some crosslinked protuberances on the surface (Fig. 3). Figure 4 indicates that after irradiation the fractured ends of the filaments turn brittle, but the fractured ends of the original filaments revealed that appearance of the facture was plastic and involved with the sliding and fracture of the macrofibrils. From Figure 4(b) it may also be observed that the irradiation-induced degradation is not uniform throughout the cross section of the filaments and varies with depth from the outer (skin) to the inner (core) part of the filaments, with more defects and voids between the two parts. This kind of nonuniform degradation was also reported frequently in the postirradiation oxidation of UHMWPE as a material for prostheses, which were always sterilized by γ-irradiation in orthopedics.[8,16,17] This degradation was attributed to either (1) the residual stresses when cooling after compression molding, (2) the nonuniform dose distribution through the sample's depth during irradiation, or (3) the nonuniform concentration of dissolved oxygen and hence the isolated peroxy radical concentration. Moreover, there is a difference in the degree of degradation between the irradiated side and the nonirradiated side, which was also found in the photooxidation of PET fiber.[18]

Effects of sunshine UV irradiation on the structure of UHMWPE fibers

Changes in average molecular weight

After UV irradiation the molecular weight of the UHMWPE decreased from the original 3,800,000 to

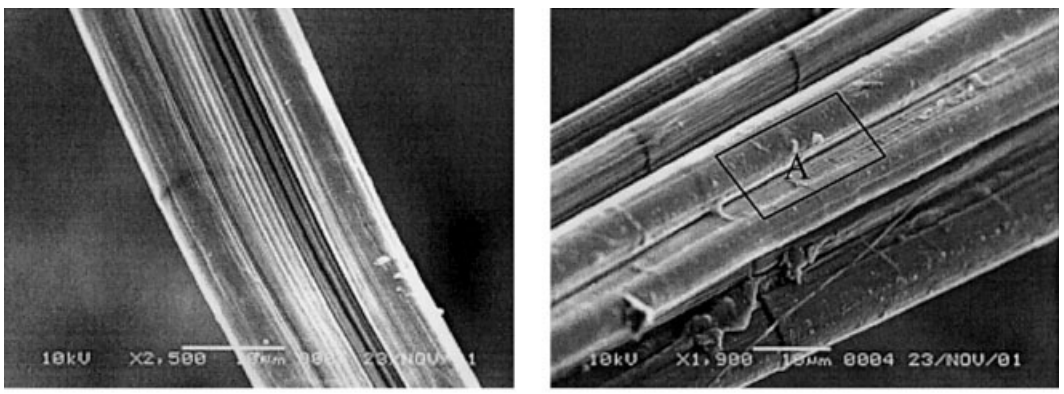

Figure 2 SEM micrographs of surfaces of SK65 filaments before (a) and after (b) irradiation.

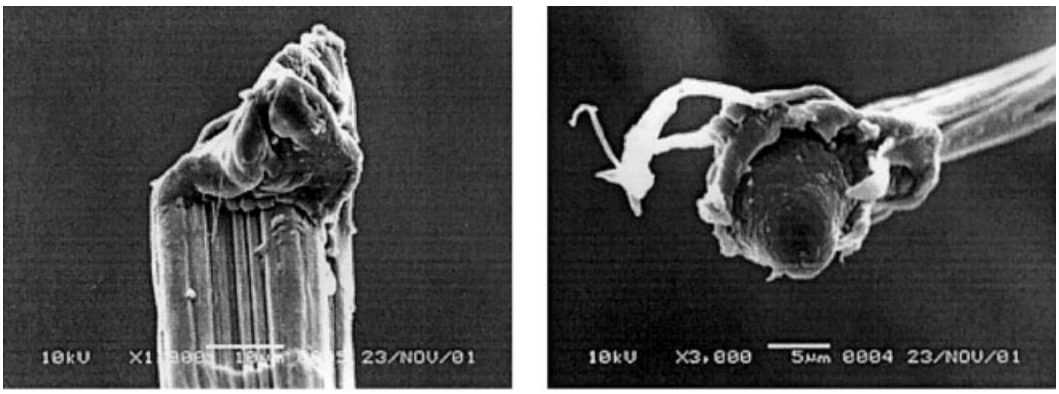

Figure 4 Tensile broken ends of SK65 filaments before (a) and after (b) irradiation.

3,100,000 after 300 h irradiation, suggesting the scission of the molecular chains. One point to note is that, although irradiation gives rise to crosslinking that can lead to the increase in tensile modulus of the filaments (Fig. 1) and the bridging of the filament surface (Fig. 3), there is no gel formation in the solution of decalin and UHMWPE, which suggests that chain scission is predominant after sunshine UV irradiation.[4]

Changes in crystalline structure

The observed diffraction peaks of UHMWPE filaments were the typical orthorhombic (110) and (200) reflections on the equatorial scans, which were characterized by 2θ at 21.79 and 24.15°, respectively. Besides these two orthorhombic reflections, there was an extra weak reflection at 19.69° that could be attributed to the monoclinic crystalline phase (001) reflection.[19] The (200) and ($20\bar{1}$) reflections of the monoclinic phase at 23.1 and 25.3° were too weak to be observable. The b-axis of the monoclinic unit cell was parallel to the molecular axis, different from the orthorhombic cell, whose c-axis was parallel to the molecular axis.[20] This monoclinic phase of polyethylene, whose appearance may be related to shear during compression,[21] usually appears under special processing conditions, such as cold working below the usual polyethylene melting point or lateral compression; higher molecular weights also favor the formation of the monoclinic phase, perhaps through its effect on the polymer mechanical relaxation spectrum.[22]

The equatorial WAXD patterns of the UHMWPE filaments before and after UV irradiation are given in Figure 5, and the calculation results are given in Table I, where FWHM is the full width at the half maximum of each crystalline peak, *CI* is the crystallinity index, and π is the crystalline orientation factor.

After UV irradiation the crystallinity of the UHMWPE fiber was increased but the crystallite size was decreased. This phenomenon was always observed after UHMWPE was irradiated with γ-rays or other high-energy electronic beams,[23–26] and was attributed to the recrystallization process with the taut-tie chain scission. The results here indicated that the same irradiation-induced taut-tie molecule scission–recrystallization mechanism also existed in the UV irradiation–induced increase in crystallinity and decrease in crystallite size, although the degree of change was negligible. The crystalline orientation was almost unchanged with UV irradiation. With recrystallization the monoclinic phase was also slightly decreased, perhaps because of the local stress relaxation of the monoclinic crystalline phase, as suggested in Seto et al.[20] There are no indications of the presence of a hexagonal phase either before or after irradiation, which would give its strongest reflection at 21.0°,[27] suggesting that the irradiation-induced crosslinking is not dominant compared with chain scissions.

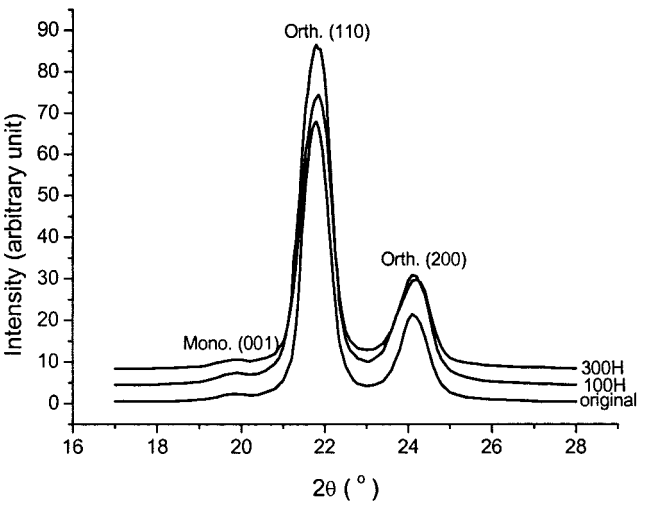

Figure 5 Equatorial WAXD diffraction patterns before and after irradiation.

TABLE I
Resolved and Calculated Equatorial Peak Parameters Before and After Irradiation

	(110)			(200)				
	2θ (°)	FWHM (°)	L_{110} (nm)	2θ (°)	FWHM (°)	L_{200} (nm)	*CI* (%)	π (%)
Original	21.7905	0.6930	11.66	24.1522	0.7394	10.98	77.45	92.4
100 h	21.7738	0.7756	10.42	24.1249	0.8442	9.62	77.76	92.1
300 h	21.7944	0.7688	10.52	24.1575	0.8178	9.93	78.13	92.7

Changes in sonic orientation

The overall chain orientation is slightly decreased from the original 0.9903 to 0.9885 after 300 h irradiation, corresponding to the scission and local relaxation of the tie molecules.

DSC analysis

The results of the DSC analysis are illustrated as Figure 6. Various investigations into the melting behavior of UHMWPE fibers showed that the DSC and/or DTA curves of UHMWPE fibers have multiple endothermic peaks,[28,29] of which the first peak was thought to result from the unconstrained fibrillar crystals and/or lamellar crystals overgrown from the shish-kebab fibrils; the second, from the melting of the orthorhombic crystallites; and the third, from the crystal–crystal phase transformation from orthorhombic to hexagonal crystals. From Figure 6 we see that the onset temperature of the melting of the orthorhombic crystals decreases because of chain scissions in the amorphous region and thus the less amorphous constraint imposed on the crystalline region; the heat of fusion increases because of the formation of C═O groups[30]; the orthorhombic–hexagonal transition temperature decreases because of the combination of the introduction of chemical defects and/or a reduction of the conformational entropy of the melt caused by the introduction of crosslinks[31]; and the melting of the hexagonal phase becomes indiscernible after irradiation. The main endotherm peak temperature remains unchanged, but its breadth is widened. This result is in agreement with reports of the nitric acid etching on the increase of heat of fusion of UHMWPE fiber as a result of molecular weight reduction[32] and with reports of low-dose Co^{60} irradiation on the unchanged melting point.[33] All results of the DSC scans suggest that chain scission and the formation of C═O chemical defects in the amorphous region are the main mechanisms of the deterioration of the UHMEPE fibers.

DMA analysis

The results of DMA analysis on the single UHMWPE filament are illustrated in Figure 7. There were numerous studies on the dynamic mechanical analysis of polyethylene with different specimen forms such as crystal mats, films, and fibers, suggesting that at least three relaxation processes can be found in different specimens with temperature sweeping.[34–37] The highest temperature mechanical loss was designated as

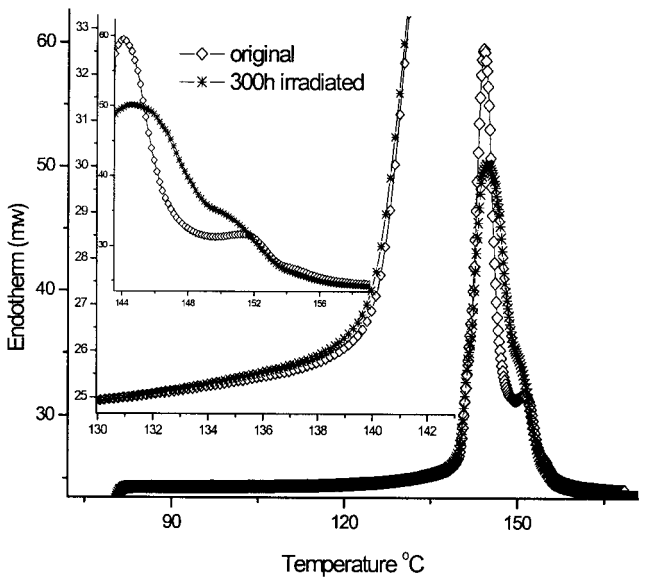

Figure 6 DSC curves of SK65 filaments before and after irradiation.

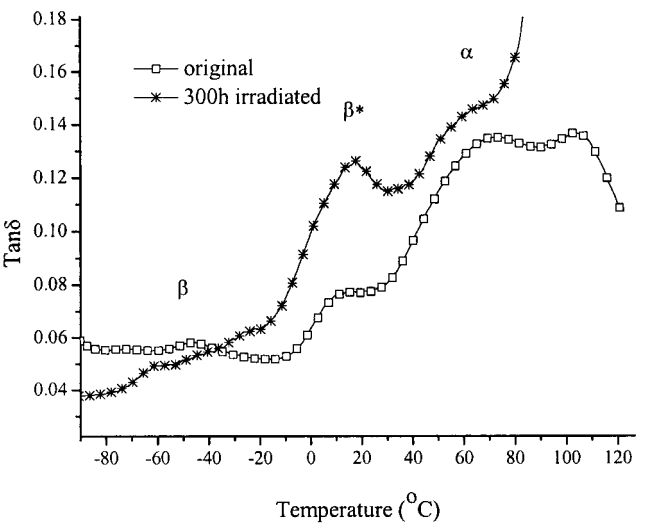

Figure 7 Plots of tan δ–temperature relationships of SK65 filament before and after irradiation.

α-relaxation, which was attributed to the molecular motions in the crystalline areas; the lowest temperature one was designated as γ-relaxation, which resulted from the local molecular motions mainly in the amorphous part and also included the contributions from the defects in the crystalline areas with the mechanism of crankshaft motions of local molecular chains; and the one between these two relaxations was designated as β-relaxation, of which the molecular interpretation was sometimes ambiguous but generally attributed to the molecular motions in the amorphous areas, and was designated as the glass transition of the specimen by some authors. Because of the constraints of crystalline areas on the amorphous areas and the high crystallinity of polyethylene, sometimes there were no, or indiscernible, β-relaxations during the DMA temperature ramp.[36]

Dependency of the loss factor (tan δ) on temperature of the unirradiated UHMWPE fiber is nearly identical to that of UHMWPE ultra-drawn single-crystal mats in Furuhata et al.[38] DMA analysis indicates that the original fiber has two β-relaxations and one α-relaxation. The peak above the temperature of α-relaxation may be attributed to the premelting of the weak point of the filament or the solid–solid orthorhombic–hexagonal transition, whose temperature is lowered by tension imposed by the DMA instrument. The β-relaxation at about -40°C originates mainly from the amorphous region of the fiber. Besides this β-relaxation, there is also a β*-relaxation at about 15°C, which was never previously observed on UHMWPE specimens other than ultradrawn fibers. Many NMR analyses[39–41]have shown (1) that UHMWPE fiber has an oriented, mobile component that consists of all-*trans* zigzag conformational molecules like the crystalline phase but with chain mobility like the amorphous phase, and (2) that this component is largely attributed to the unique fiber structure attained on gel spinning. Judging from its imperfect lateral packing and chain mobility, it is reasonable to assign β*-relaxation to molecular motions of the oriented mobile component.

From Figure 7 we see that after irradiation the β-relaxation has been broadened and becomes unsymmetrical because of the scission and oxidation of the main chains; the former will lower the temperature and the latter will increase the temperature of the β-relaxation. The increase of the intensity of the α-relaxation is attributable to the increase of constraints imposed by the amorphous regions resulting from the oxidation of the material. The most obvious change is in the β*-relaxation, whose transition temperature and intensity were increased by UV irradiation.

CONCLUSIONS

After sunshine-simulated UV beam irradiation, the tenacity, break extension, and work to break of the UHMWPE fibers were conspicuously decreased as a result of chain scission, and the modulus was slightly increased, suggesting molecular crosslinking. A change from ductile to brittle fracture mechanism was found after UV irradiation. The molecular weight measurement showed that chain scission was dominant. The crystallinity of UHMWPE fibers increased slightly and the crystallite size decreased on UV irradiation by the mechanism of local scission–recrystallization. Crystalline orientation changed only slightly, although the overall sonic molecular orientation decreased after irradiation. After irradiation the intensity and temperature of the β- and α-relaxations changed, although less obviously than the β*-relaxation, suggesting that the UV irradiation–induced degradation was located primarily at the amorphous and the interface areas of the UHMWPE fiber, where the crystalline areas scarcely changed. Besides, SEM observations indicate the UV-induced degradation was nonuniform through the cross section of the UHMWPE filaments, with the surface seriously degraded and the core slightly deteriorated, suggesting that degradation is a diffusion-controlled process. Finally, the degradation was spatially nonuniform, with the directly irradiated side more degraded than the nonirradiated side.

References

1. Rabek, J. F. Polymer Photodegradation: Mechanisms and Experimental Methods; Chapman & Hall: London, 1995; p. 577.
2. Rabek, J. F. Mechanisms of Photophysical Process and Photochemical Reactions in Polymers: Theory and Applications; Wiley: New York, 1987; pp. 484–490.
3. Scott, G. In: Ultraviolet Light Induced Reactions with Polymers; Labana, S. S., Ed.; ACS Symposium Series 25; American Chemical Society: Washington, DC, 1976; p. 340.
4. Rabek, J. F. Photodegradation of Polymers: Physical Characteristics and Applications; Springer-Verlag: Berlin, 1996; pp. 98–107.
5. Ranby, B.; Rabek, J. F. Photodegradation: Photo-oxidation and Photostabilization of Polymers; Wiley: New York, 1975.
6. Gsell, R. A.; Stein, H. L.; Ploskonka, J. J. Characterization and Properties of Ultra-high Molecular Weight Polyethylene; ASTM STP 1307; ASTM: Scranton, PA, 1998.
7. Kurtz, S. M.; Muratoglu, O. K.; Evans, M.; Edidin, A. A. Biomaterials 1999, 20, 1659.
8. O'Neill, P.; Birkinshaw, C.; Leahy, J. J.; Buggy, M.; Ashida, T. Polym Degrad Stab 1995, 49, 239.
9. Khanna, Y. P.; Turi, E. A.; Taylor, T. J. Macromolecules 1995, 18, 1303.
10. Mead, W. T.; Desper, C. R.; Porter, R. J Polym Sci Part B: Polym Phys 1979, 17, 859.
11. Murthy, N. S.; Minor, H. Polymer 1990, 31, 996.
12. Hsieh, Y. L.; Hu, X. P. J Polym Sci Part B: Polym Phys 1997, 35, 623.
13. Nakame, K.; Nishino, T.; Ohkubo, H. J Macromol Sci Phys 1991, B30, 1.
14. Xiao, H.; Zhang, Y.; An, S.; Jia, G. J Appl Polym Sci 1996, 59, 931.
15. Hsieh, Y. L.; Barrall, G.; Xu, S. J Appl Polym Sci 1992, 33, 536.
16. Yeom, B.; Yu, Y. J.; Mckellop, H. A.; Salovey, R. J Polym Sci Part A: Polym Chem 1998, 36, 333.

17. Eyerer, P.; Ke, Y. C. J Biomed Mater Res 1984, 18, 1137.
18. Ruetsch, S. B.; Huang, X. X.; Salem, D. R.; Weigmann, H. D. Textile Res J 1996, 66, 185.
19. Moonen, J. A. H. M.; Roovers, W. A. C.; Meierand, R. J.; Kip Bert, J. J Polym Sci Part B: Polym Phys 1992, 30, 361.
20. Seto, T.; Hara, T.; Tanaka, K. Jpn J Appl Phys 1968, 7, 31.
21. Rastogi, S.; Kurelec, L.; Lemstra, P. J. Macromolecules 1998, 31, 5022.
22. Desper, C. R.; Cohen, S. H.; King, A. O. J Appl Polym Sci 1993, 47, 1129.
23. Bhateja, S. K.; Andrew, E. H.; Young, R. J. J Polym Sci Part B: Polym Phys 1983, 21, 523.
24. Shinde, A.; Salovey, R. J Polym Sci Part B: Polym Phys 1985, 23, 1681.
25. Tretinnikov, O. N.; Ogata, S.; Ikada, Y. Polymer 1998, 39, 6115.
26. Premnath, V.; Bellare, A.; Merrill, E. W.; Jasty, M.; Harris, W. H. Polymer 1999, 40, 2215.
27. Basset, D. C.; Block, J.; Piermarini, G. J. J Appl Phys 1974, 45, 4146.
28. Hsieh, Y. L.; Ju, J. J Appl Polym Sci 1994, 53, 347.
29. Khosravi, N.; Warner, S. B.; Murthy, N. S.; Kumar, S. J Appl Polym Sci 1995, 57, 781.
30. Sebaa, M.; Servens, C.; Pouyet, J. J Appl Polym Sci 1992, 45, 1049.
31. Hoogsteen, W.; Brinke, G. T.; Pennings, A. J. Colloid Polym Sci 1988, 266, 1003.
32. Khosravi, N.; Warner, S. B. Murthy, N. S.; Kumar, S. J Appl Polym Sci 1995, 57, 781.
33. Zhao, Y.; Luo, Y.; Jiang, B. J Appl Polym Sci 1993, 50, 1797.
34. Boyd, R. H. Polymer 1985, 26, 323.
35. Boyd, R. H. Polymer 1985, 26, 1123.
36. Roy, S. K.; Kyu, T.; Manley, R. S. J. Macromolecules 1988, 21, 1741.
37. Matsuo, M.; Sawatari, C.; Ohhata, T. Macromolecules 1988, 21, 1317.
38. Furuhata, K.; Yokokawa, T.; Miyasaka, K. J Polym Sci Part B: Polym Phys 1984, 22, 133.
39. Chen, W.; Fu, Y.; Wunderlich, B.; Cheng, J. J Polym Sci Part B: Polym Phys 1994, 32, 2661.
40. Kaji, A.; Ohta, Y.; Yasuda, H.; Murano, M. Polym J 1990, 22, 455.
41. Tzou, D.-L.; Huang, T.-H.; Abhiraman, A. S.; Desai, P. Polymer 1992, 33, 426.